Physica Scripta. Vol. T115, 915–917, 2005

Ca-UO_2-CO_3 Complexation – Implications for Bioremediation of U(VI)

S. D. Kelly[1*], K. M. Kemner[1], S. C. Brooks[2], J. K. Fredrickson[3], S. L. Carroll[2], D. W. Kennedy[3], J. M. Zachara[3], A. E. Plymale[3] and S. Fendorf[4]

[1]Environmental Research Division, Argonne National Laboratory, 9700 South. Cass Ave, Argonne, IL, USA
[2]Oak Ridge National Laboratory, Oak Ridge, TN, USA
[3]Pacific Northwest National Laboratory, Richland, WA, USA
[4]Stanford University, Stanford, CA, USA

Received June 26, 2003; accepted January 8, 2004

PACS numbers: 01.30.Cc, 61.10.Ht, 82.30.Nr

Abstract

An attractive remediation strategy for the removal of highly soluble U(VI) from groundwater is microbial reduction of soluble U(VI) to U(IV) as insoluble uraninite. The feasibility of this remediation strategy depends on the rate and extent of microbial reduction of U(VI) in the presence of ions commonly found in groundwater that can form complexes with uranyl. Recently, Ca in solutions with U(VI) has been shown to inhibit microbial reduction of U(VI). Indirect evidence supports the formation of a Ca-UO_2-CO_3 complex that may be responsible for the limited microbial reduction of U(VI) in the presence of Ca, but direct evidence for the formation of a Ca-UO_2-CO_3 complex is needed for verification. X-ray absorption fine-structure measurements of solutions containing 50 μM U(VI) and 30 mM bicarbonate, with and without 5 mM Ca, were made to determine whether a Ca-UO_2-CO_3 complex was present. These results are discussed.

1. Introduction

Activities associated with the mining and processing of U ores have resulted in vast areas of environmental contamination. Current remediation strategies are based on the removal of soluble U(VI) from the aqueous phase by reducing it to insoluble U(IV) in the form of a uranium oxide precipitate, uraninite. The formation of the insoluble uraninite should minimize the transport of U from contaminated areas. Previous studies have shown that dissimilatory metal-reducing bacteria (DMRB) couple the oxidation of organic matter or of H_2 to the reduction of oxidized metals including U(VI). The feasibility of this remediation strategy depends on the rate and extent of microbial reduction of U(VI) in the presence of ions commonly found in groundwater that can form complexes with U(VI).

Factors that enhance or inhibit bacterial U(VI) reduction are not well understood. Recently, Ca in solutions with U(VI) has been shown to inhibit microbial reduction of U(VI) [1]. Indirect evidence of for a Ca-UO_2-CO_3 solution complex in solution has been demonstrated [2, 3]. Such complexes have been largely overlooked, because most equilibrium speciation models predict the dominant uranyl species in calcareous groundwater to be uranyl carbonates. These species may be responsible for the limited microbial reduction of U(VI). Direct evidence for the formation of a Ca-UO_2-CO_3 complex is needed to help clarify the cause of the limited microbial reduction of U(VI) in calcareous groundwater.

X-ray absorption fine-structure (XAFS) measurements of solutions containing environmentally relevant concentrations of U(VI) (50 μM), bicarbonate (30 mM), and acetate (5 mM) with and without Ca (5 mM) have been made to determine the presence of a Ca-UO_2-CO_3 complex. Our previous study [1] briefly reported results for a similar +Ca solution (with no added acetate) as supporting evidence for the formation of a Ca-UO_2-CO_3 complex. A more thorough analysis of the EXAFS data from two samples that differ only in the presence or absence of Ca is presented here.

2. Experimental Methods

The solution samples were prepared under anoxic conditions. Both solution samples contain 50 μM U(VI), 30 mM HCO_3, and 5 mM acetate. One sample (+Ca) also contains 5 mM $CaCl_2$ while the other sample (−Ca) did not. The U concentration in these samples of 50 μM are similar to the level of U contamination at the NABIR Field Research Center site, Oak Ridge National Laboratory, TN, USA, but are very dilute for EXAFS measurements. For our 3 mm thick sample the change in the absorption coefficient at the U L_3-edge is approximately 2×10^{-4}. This edge step is approximately two orders of magnitude smaller than a standard edge step for a fluorescence measurement. Uranium L_3-edge EXAFS measurements were made at the MR-CAT insertion device (10-ID) beamline [4] at the Advance Photon Source. The insertion device was tapered to reduce the variation in the X-ray intensity (to less than 15%) through the scanned energy range. A Si(111) double crystal monochromator was used to select the X-ray energy. A Rh mirror was used to remove X-rays with higher harmonic energies. The measurements were made in fluorescence mode by using a 13 element solid-state detector (Canaberra with XIA electronics). The incident X-ray intensity was monitored using a nitrogen filled ion chamber. The intensity of the nonfocused beam of approximately 1 mm square at the U L_3-edge is approximately 5×10^{13} photons/s. The integration time for each data point of approximately 12 s resulted in approximately one EXAFS scan per hour. The +Ca sample was scanned 3 times while the −Ca sample was scanned 10 times. The data were processed by using standard procedures and with UWXAFS [5] software package. The averaged $\chi(k)$ data are shown in Figure 1. Theoretical models were constructed with the program FEFF7 [6] and the crystallographic atomic positions of andersonite [7]. Automatic overlap of the muffin tin potentials was used in the FEFF7 calculation as previously reported [8].

*e-mail: skelly@anl.gov

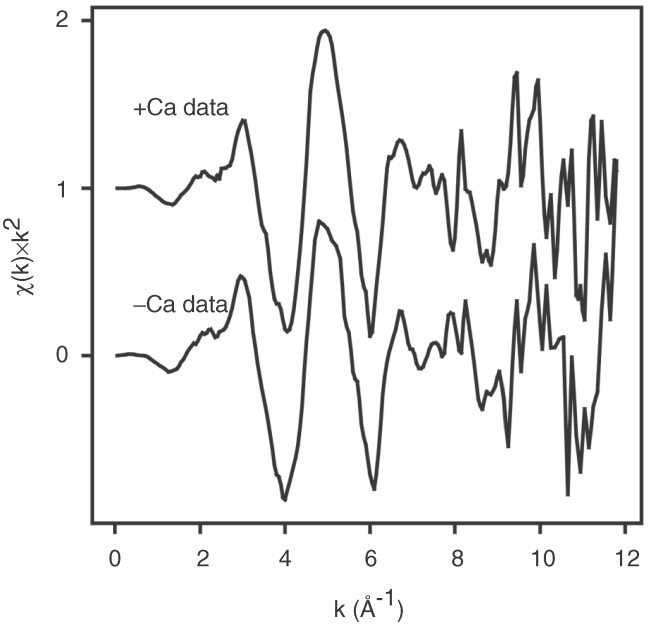

Fig. 1. Averaged $\chi(k) \cdot k^2$ data from the +Ca (2.7 to 10 $Å^{-1}$) and −Ca (2.7 to 9 $Å^{-1}$) samples.

3. EXAFS Data Analysis

Speciation calculations based on formation constants for a proposed Ca-UO_2-CO_3 complex indicated that this complex will be the major (∼98.4%) component in our +Ca sample [1]. The U(VI) is in the form of a uranyl tricarbonate species with an unknown number of Ca atoms, presumably bound to the distant oxygen atoms of the carbonate groups. A ball-and-stick model of this species is shown in Fig. 2. This figure shows the equatorial oxygen (Oeq) atoms in the plane of the page with the axial oxygen (Oax) atoms above and below the uranium atom. The model for this structure contains 4 shells of atoms. The coordination numbers in the model for the uranyl-tricarbonate species are held to the expected values based on the speciation calculations. These coordination numbers are 2 Oax, 6 Oeq, 3 C, and 3 Odist (distant oxygen atoms of the carbonate groups) as shown in Fig. 2.

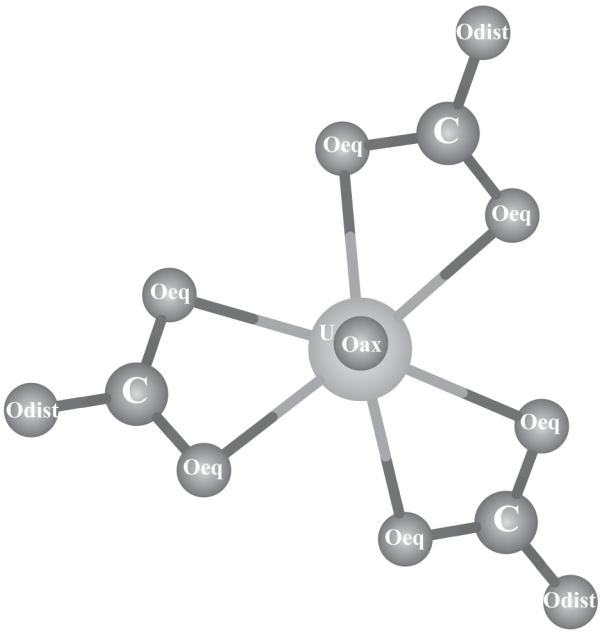

Fig. 2. Ball and Stick figure of $(UO_2)(CO_3)_3$ species. The uranyl moiety (UO_2^{2+}) is made up of the U atom bound with two axial oxygen (Oax) atoms that are located above and below the U atom.

Important U-Oax1-U-Oax2 and U-C-Odist multiple scattering (MS) paths that must be included in the model. The EXAFS variables for these MS paths can be approximately parameterized in terms of the single scattering (SS) path containing the end atoms. For a linear group of three atoms, U-C-Odist, the σ^2-value of the SS path U-Odist has been set equal to the σ^2-value of the MS paths. This is exactly true if the atoms are linear and becomes an approximation as they deviate slightly from linearity. The σ^2-values for the U-Oax1-U-Oax2 MS paths are parameterized as described elsewhere [8]. Based on other Ca-UO_2-CO_3 systems, the U-Ca distance is expected to be about 3.8 to 4.1 Å. This path was added to model our +Ca data. Table I lists the paths included in the model and the EXAFS parameterizations.

Both data sets (+Ca and −Ca) were fit simultaneously by using a k-weight values of 1, 2, and 3 in the Fourier transform. Initially all N, Δr and σ^2 values were constrained to the same values for both data sets. This initial model failed to reproduce both data sets simultaneously. The other extreme, allowing all N, Δr and σ^2 values to vary independently also failed because of our limited data ranges. The minimum freedom needed to describe the data accurately was determined to have equal N and Δr values for both data sets and variable σ^2 values (See Table I).

Table I. *EXAFS parameters for the simultaneous fits to +Ca and −Ca data sets. One S_0^2 value and one ΔE value were also determined in the fit. The two data sets have 6 common variables ($\Delta Roax$, $\Delta Roeq$, ΔRc, $\Delta Rodist$, ΔE, and S_0^2). The −Ca data set has 4 (σ^2oax-, σ^2oeq-, σ^2c-, and $\sigma^2odist-$) independent variables, while the +Ca data set has 7 (σ^2oax+, σ^2oeq+, σ^2c+, $\sigma^2odist+$, $Nca+$ $\Delta Rca+$, and σ^2ca+) independent variables. Therefore, the −Ca and +Ca data sets have averages of 7 and 10 variables, respectively. The −Ca and +Ca data sets have 14 and 16 independent points, respectively. The M.S. path U-C-Odist has a degeneracy of twice the S.S. path U-Odist because there are two equivalent M.S. paths (U-Odist-C and U-C-Odist).*

Path	Model	N	ΔR	σ^2
U-Oax	+Ca	2	$\Delta Roax$	σ^2oax+
	−Ca			σ^2oax-
U-Oeq	+Ca	6	$\Delta Roeq$	σ^2oeq+
	−Ca			σ^2oeq-
U-C	+Ca	3	ΔRc	σ^2c+
	−Ca			σ^2c-
U-Oax1-U-Oax1	+Ca	2	$2 \cdot \Delta Roax$	$4 \cdot \sigma^2oax+$
	−Ca			$4 \cdot \sigma^2oax-$
U-Oax1-Oax2	+Ca	2	$2 \cdot \Delta Roax$	$2 \cdot \sigma^2oax+$
	−Ca			$2 \cdot \sigma^2oax-$
U-Oax1-U-Oax2	+Ca	2	$2 \cdot \Delta Roax$	$2 \cdot \sigma^2oax+$
	−Ca			$2 \cdot \sigma^2oax-$
U-Ca	+Ca	$Nca+$	$\Delta Rca+$	σ^2ca+
U-Odist	+Ca	3	$\Delta Rodist$	$\sigma^2odist+$
	−Ca			$\sigma^2odist-$
U-C-Odist	+Ca	6	$\Delta Rodist$	$\sigma^2odist+$
	−Ca			$\sigma^2odist-$
U-C-Odist-C	+Ca	3	$\Delta Rodist$	$\sigma^2odist+$
	−Ca			$\sigma^2odist-$

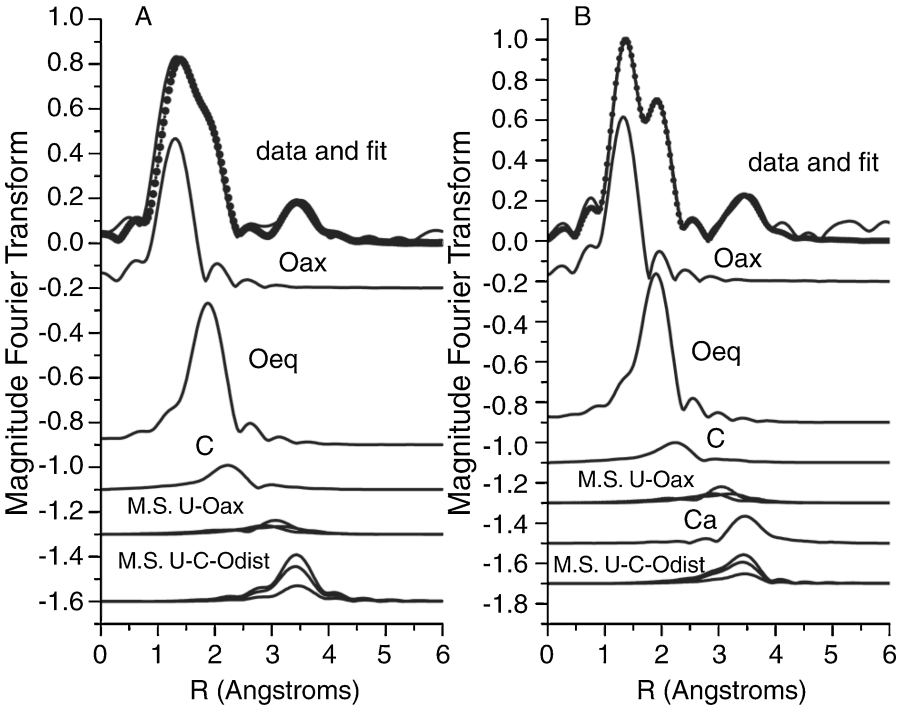

Fig. 3. The magnitude of the Fourier transform of the −Ca (A) and +Ca (B) data and the model using a *k*-weight of 2. The top of each panel shows the data (line) and the fit (symbols). Beneath the data and fit are the individual contributions to the model from each path. The fit range is 1 to 4 Å.

Table II. *Best-fit values from the simultaneous fit of +Ca and −Ca data. Values without uncertainties were not determined in the fit to the data. The best-fit value for S_0^2 is 0.83 ± 0.10 and ΔE is 5.3 ± 0.8 eV for all paths of both data sets.*

Path	Data Set	*N*	*R* (Å)	σ^2 ($\times 10^{-3}$ Å^2)
U-Oax	+Ca	2	1.82 ± 0.01	0 ± 1
	−Ca			1 ± 1
U-Oeq	+Ca	6	2.45 ± 0.01	5 ± 1
	−Ca			7 ± 2
U-C	+Ca	3	2.88 ± 0.03	12 ± 6
	−Ca			10 ± 8
U-Oax1-U-Oax1	+Ca	2	3.64 ± 0.01	0 ± 1
	−Ca			5 ± 5
U-Oax1-Oax2	+Ca	2	3.64 ± 0.01	0 ± 1
	−Ca			3 ± 3
U-Oax1-U-Oax2	+Ca	2	3.64 ± 0.01	0 ± 1
	−Ca			3 ± 3
U-Ca	+Ca	1.4 ± 1.2	4.02 ± 0.03	0 ± 1
U-Odist	+Ca	3	4.11 ± 0.02	8 ± 10
	−Ca			3 ± 3
U-C-Odist	+Ca	6	4.11 ± 0.02	8 ± 10
	−Ca			3 ± 3
U-C-Odist-C	+Ca	3	4.11 ± 0.02	8 ± 10
	−Ca			3 ± 3

Figure 3 shows the Fourier transform of the data and the best-fit models. Under the data and model in the Figure 3 is shown the individual contribution from each path included in the models, illustrating the importance of the MS paths and the overlap of the Odist paths with the Ca path. The best-fit values for all the paths included in the models are listed in Table II.

4. Conclusions

The best-fit value for the number of Ca atoms for the +Ca sample is 1.4 ± 1.2 indicating the presence of a Ca-UO_2-CO_3 complex in this sample. All the other parameters including the σ^2 values and Δr values, are within the uncertainties of previously reported values. Simultaneously fitting the +Ca and −Ca data was necessary to distinguish between the contribution from the Ca atom, the distant oxygen (Odist), and the MS paths (U-C-Odist) of the carbonate groups. Direct evidence of the Ca-UO_2-CO_3 complex and its role in bioreduction of U(VI) in calcareous ground waters like those found at the FRC must be considered in developing a feasible bioremediation strategy.

Acknowledgment

Use of the Advanced Photon Source and MRCAT was supported by the U.S. Department of Energy, Office of Science, Office of Basic Energy Sciences, under Contract No. W-31-109-ENG-38. The work was supported by the U.S. Department of Energy, Office of Science, Office of Biological and Environmental Research, Natural and Accelerated Bioremediation Program.

References

1. Brooks, S. C., *et al.*, Environ. Sci. Technol. **37**, 1850 (2003).
2. Kalmykov, S. N. and Choppin, G. R., Radiochim. Acta **88**, 603 (2000).
3. Bernhard, G., Geipel, G., Brendler, V. and Nitsche, H., Radiochim. Acta **74**, 87 (1996).
4. Segre, C. U., *et al.*, Synchrotron Radiation Instrumentation: Eleventh U.S. Conference **CP521**, 419 (2000).
5. Stern, E. A., Newville, M., Ravel, B., Yacoby, Y. and Haskel, D., Physica B **208 & 209**, 117 (1995).
6. Zabinsky, S. I., Rehr, J. J., Ankudinov, A., Albers, R. C. and Eller, M. J., Phys. Rev. B **52**, 2995 (1995).
7. Coda, A., Della Giusta, A. and Tazzoli, V., Acta Cryst. **B37**, 1496 (1981).
8. Hudson, E. A., Rehr, J. J. and Bucher, J. J., Phys. Rev. B **52**, 13815 (1995).